NUMERICAL STUDY OF COLLAPSE BEHAVIOR OF RC BRIDGES DUE TO EXTREMELY HIGH SEISMIC LOAD CONSIDERING POST-PEAK BEHAVIOR

Tekehiro KURODA[1] and Kimiro MEGURO[2]

ABSTRACT: The analytical model for collapse analysis which is taken into account for the effect of post-peak behavior due to reinforcement buckling and concrete spalling is developed based on the Applied Element Method (AEM). A multi-span bridge was simulated using the proposed model. The analysis result shows a bridge pier designed according to 1964 Japan's seismic design code has brittle shear failure mode and suffer much damage if it is subjected to the level 2 earthquake ground motion specified in Japan's current seismic design code. In addition, the bridge pier designed according to current seismic design code does not collapse although it is subjected to an extremely high seismic earthquake ground motion. However, a large relative displacement between a pier and deck results in deck falling.

Key Words: Collapse analysis, Post-peak behavior, Extremely high seismic load

INTRODUCTION

In order to mitigate the casualties due to structural collapse during an earthquake, seismic performance for each structure should be evaluated. Because structural performance is assigned during the design period and the design varies considerably with the input load, the structural seismic performance is significantly affected by the designed input ground motion. In general, an earthquake ground motion for a structure is considered from both occurrence probability and cost-effectiveness. However, at present, it is impossible to fully guarantee that the designed ground motion is one of the most vulnerable and probable earthquakes for a structure to resist. Moreover, it is likely that the real earthquake ground motion occurring during the lifetime of the structure will cause seismic loads to exceeding the design level. In this case, the performance of the structures should also be sufficiently predicted to ensure that the structure will not cause damages to the society. In order to satisfy the criteria, it is inevitable to develop the effective means to predict the behavior of structure from the initial state to total collapse.

For a rational assessment of seismic performance, an analytical method for predicting the post-peak response of the RC structure is needed. During strong earthquakes, RC members subject to cyclic loading may experience a very large deformation into a post-peak range. Consequently, the longitudinal reinforcement may deform laterally, which is known as buckling while cover concrete may spall off due to large compressive strains. From experiments conducted in the past on laterally loaded RC columns (Fukui et al. 1998), considerable softening behavior is attributable to the spalling of cover concrete and buckling of longitudinal reinforcement. Hence, for a rational evaluation of

[1] Graduate student
[2] Associated professor

post-peak seismic performance of RC structures, stress-strain relationships of concrete and reinforcing steel, including spalling and buckling mechanisms, are required (Maekawa 2003).

This paper studies the behavior of reinforced concrete structure subjected to an external earthquake ground motion that exceeds the design earthquake level. The selected numerical model in this study has the capability to capture the behavior of structure from an elastic range to a total collapse. The model was improved so that it can capture the post-peak behavior by taking into account the effect of concrete spalling and reinforcement buckling. The analysis result is verified with the quasi-static cyclic loading test. Last, the model has been applied to simulate behavior of multi-span bridge under the extremely high earthquake ground motion.

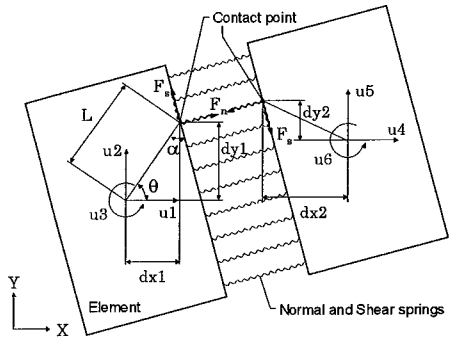

Figure 1. Element shape, Contact Point and Degree of Freedom

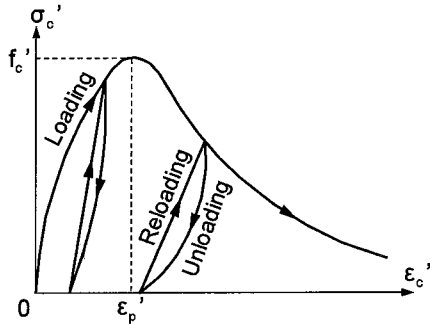

Figure 2. Cyclic compressive stress-strain relationship for concrete

OUTLINE OF THE PROPOSED ANALYTICAL MODEL

Review on the Applied Element Method (AEM)

AEM (Meguro 2000) is a recently developed numerical model that can follow structural behavior from an elastic range to a total collapse. In AEM, a structure is modeled as an assembly of small rigid elements connected together with a zero-length normal and shear spring as shown in Figure 1. At the location of rebar, the spring properties are modified by increasing the value of stiffness and strength so that the spring represents both reinforcement and concrete at that position. The governing equation regarding the displacement and the external force of each element in a static analysis is shown in the following equation:

$$K\Delta U = \Delta F \tag{1}$$

where K is structural stiffness matrix, DU is incremental displacement vector and ΔF is incremental force vector. This formula is the same as stiffness equation in stiffness method for structural analysis. The governing equation written in the incremental form in dynamic analysis is shown below:

$$\left[\frac{1}{\beta(\Delta t)^2}M+\frac{\gamma}{\beta\Delta t}C+K\right]\Delta U=\Delta F+\left[\frac{1}{\beta\Delta t}M+\frac{\gamma}{\beta}C\right]\dot{U}+\left[\frac{1}{2\beta}M+\left(\frac{\gamma}{2\beta}-1\right)\Delta tC\right]\ddot{U} \tag{2}$$

where M is mass matrix, C is damping matrix, Δt is time increment, $\dot{U}$ is velocity vector and $\ddot{U}$ the accelerating vector. After a concrete cracking, the spring at the crack position is removed. When two elements come into contact after a crack, transmission force is considered by an additional contact spring at the contact location.

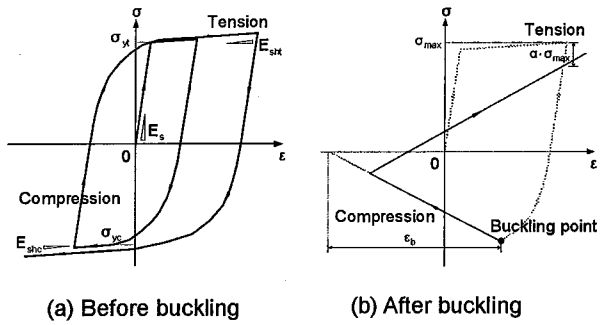

(a) Before buckling (b) After buckling

Figure 3. Stress-strain relationship for reinforcing bar

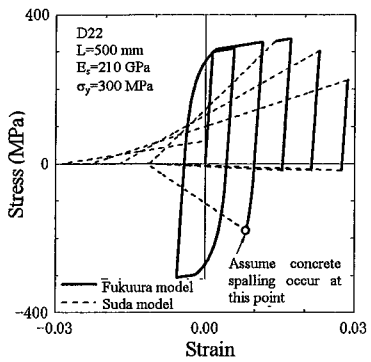

Figure 4. Stress-strain relationship for reinforcing bar after combining buckling effect

The constitutive relationship for concrete before concrete spalling

In this study, the stress-strain relationship proposed by Maekawa (2003) as shown in Figure 2 is employed for springs under compressive force model. For concrete springs subjected to tensile force, its stiffness is assumed as the initial compressive stiffness until the force reaches the tensile strength; then cracking is assumed. After cracking, spring tensile stiffness is assumed to be zero.

Determination of cover concrete spalling

When a flexural RC member is subjected to high moment, the cover concrete in the compression side suddenly spalls off and loses its load-carrying capacity. To consider the effect of concrete spalling, an equation used to predict the plastic spalling strain (ε_{sp}) proposed by Dhakal and Maekwa (1999) is adopted:

$$\varepsilon_{sp} = \varepsilon_y + \frac{a_{cr}^{\ 2}\pi^2}{4L^2} \tag{3}$$

where ε_y is yield strain of reinforcing bar nearby cover concrete, a_{cr} is the critical lateral deformation to cause complete spalling of concrete cover (Maekawa 2003) and L is bucking length which is given in Equation (4) in the next section. After concrete spalling occurred, it is assumed that no compressive or tensile force can be transferred through this concrete portion.

Constitutive relationship for reinforcing steel before buckling

When reinforcing steel is subjected to cyclic loading in the inelastic range, the yield plateau is suppressed and the stress-strain curve exhibits the Bauschinger effect, in which nonlinear response develops at a strain much lower than the yield strain. Because the Bauschinger effect is considered to have a high influence in reinforcement buckling, the Fukuura and Maekawa's multi-surface plasticity model (Fukuura 1999) which can predict the Bauschinger effect with high accuracy was chosen in this study (Figure 3a). This model can represent the internal loops with the same accuracy as Kato's model (Kato 1979) but with considerable reduction in path-dependent parameters. In the model, the reinforcing bar is assumed to consist of numerous microscopic elements by a serial connection of the elastic springs and plastic sliders. Therefore, Bauschinger effect is naturally obtained by assigning different yield strengths to plastics sliders.

Determination of buckling length

The formula used to determine reinforcement the buckling length in this study was first proposed by Suda et al. (1999). Later, the formula has been modified by considering the effect of non-linearity in reinforcement by Asatsu et al. (2001). The formula for determining the reinforcement buckling

length (L_{cr}) is shown in the following equation:

$$L_{cr} = 8.5\sigma_{sy}^{4/5}\beta_n^{-1/3}\phi \quad (4)$$

where σ_{sy} is yield stress of longitudinal reinforcing bar, ϕ is reinforcement diameter and β_n is stiffness against reinforcing bar buckling which is taken into account for confinement effect due to tie reinforcements and cover concrete.

The Constitutive relationship for reinforcing steel after buckling

Suda's model (Suda et al. 1999) is adopted for the stress-strain relationship after reinforcing bar buckling. This model considers the compression drop after reinforcement buckling and re-tension behavior as a straight line (Figure 3b). By combining Suda's model for buckling reinforcement and Fukuura and Maekawa's model, the complete stress-strain relationship for reinforcing bar including reinforcement buckling is obtained as shown in Figure 4. This model was used through this study to study the effect of reinforcement buckling. The whole procedure for calculating the stress-strain relationship including buckling effect in this study is shown in Figure 5.

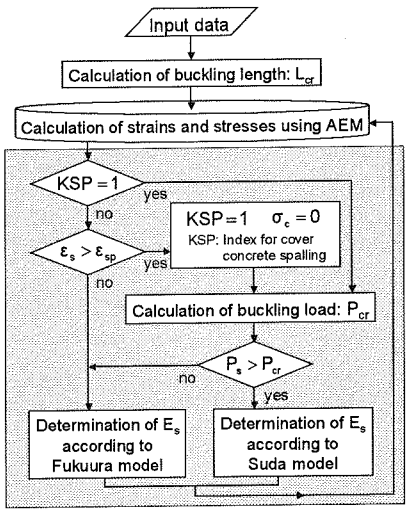

Figure 5. Flowchart for calculating force and deformation in reinforcing bar including buckling effect

VERIFICATION

Quasi-static cyclic loading test and analytical model description

To verify the proposed model, analytical results were compared with the quasi-static cyclic loading test (Yoshikawa 1997). The detail of the test specimen is summarized in Table 1 and Figure 6. From the experimental result (Figure 9), the deterioration in peak resisting force was observed when the lateral displacement at the top of the pier is equal to 7 δ_y (yielding displacement). Moreover, the starting of concrete spalling was also found at this displacement level. Therefore, it is expected that the cause in strength deterioration is mainly resulted from reinforcement buckling. For the analytical model (Figure 7), the total number of 512 element of 2-dimension 4x4 cm^2 squared shape was selected to represent the specimen.

Comparison and discussion

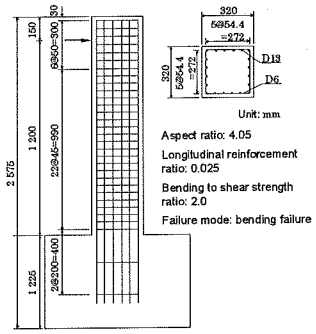

Figure 6. Dimension and reinforcement Detail of test specimen

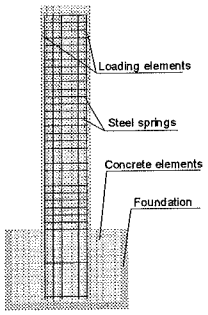

Figure 7. Dimension and reinforcement Detail of analytical model

Table 1. Material properties for test specimen

Concrete	Compressive strength (MPa)	28.4
	Young's modulus (GPa)	20.4
Longitudinal reinforcement	Yield strength (MPa)	356
	Young's modulus (GPa)	187
Tie reinforcement	Yield strength (MPa)	444
	Young's modulus (GPa)	192

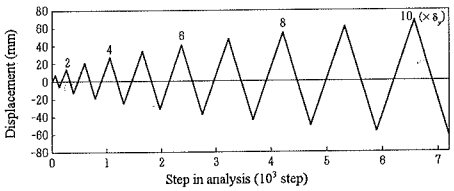

Figure 8. Cyclic load history

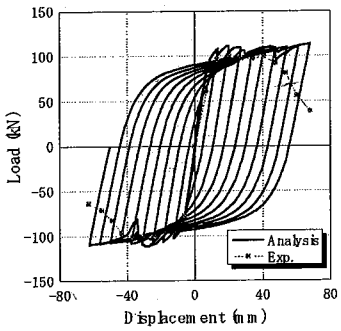

Figure 9. Comparison between test and analysis result (without buckling effect)

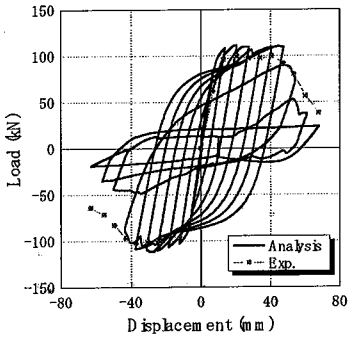

Figure 10. Comparison between test and analysis result (with buckling effect)

Load-displacement relationships obtained from analytical results with and without including the effects of concrete spalling and reinforcement buckling were plotted and compared to test the hysteretic envelop in Figures 9 and 10. The hysteretic envelop obtained from the test in the previous section was also plotted in both figures to be compared. Both models can simulate the experimental result well until the top pier displacement is 40 mm. However, beyond this point, the analytical result without the effect of concrete spalling and reinforcement buckling cannot capture the reduction of strength. The much better analytical result can be seen in Figure 6 when concrete spalling and reinforcement buckling are included.

SEISMIC PERFORMANCE EVALUATION OF THE MULTI-SPAN BRIDGE USING A PROPOSED MODEL

Prototype and analytical model description

The multi-span bridge system is consisted of three continuous spans of steel sheet decks (Figure 11). The piers were designed using 2 Japan's seismic design code in 1964 and 1996 (JSCE 2002). These two piers are referred later as pier S39 and H8, respectively. Reinforcement in each pier is shown in Figure 12. In this problem, prototype is simulated using a 3-dimensional cubic element.

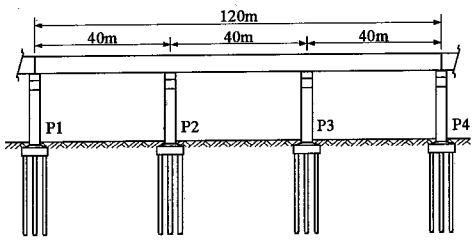

Figure 11. Dimension of multi-span bridge prototype

Input ground motion

The first ground motion used in this study was selected from the near-field ground motion equivalent to a level 2 earthquake motion specified in Japan's seismic design code in 1996 which is the life safety level (Yoneda et al. 1993). This earthquake is referred later as earthquake motion L2a. Moreover, in this study, the earthquake ground motion L2b expected to be more severe to the multi-span bridge and represented extremely high seismic load was also considered. From the acceleration response spectrum shown in Figure 13, the earthquake ground motion L2b was selected by the authors to be almost resemble the L2a except from that it has higher components in the range of period 1 sec.

Seismic performance evaluation with a static analysis

In this section, a pushover analysis was carried out. Load was horizontally applied at the upper deck position in the direction that the pier section possesses the maximum moment of inertia. The analysis result is shown in Figure 14. The circle mark indicates the point in which yielding of reinforcement starts. Dotted lines indicate the recommended force-displacement relationship from the current

standard. The analytical result shows that the starting points of reinforcement yielding match well with the design standard recommendation however the ultimate strength obtained from both piers (H8 and S39) is much higher. This can be explained as the model used in a design standard assuming that all reinforcement yields at the location of first yielding while, in the proposed model, reinforcement is gradually yielded one by one. It should be noted that the difference between ultimate strength from the analytical model and the design standard recommendation in pier S39 is several times higher than that of H8. This is not surprising as pier H8 contains a higher amount of reinforcement and fail by concrete spalling and reinforcement buckling due to the bending mode while pier S39 fails due to brittle shear failure before all longitudinal reinforcement can yield.

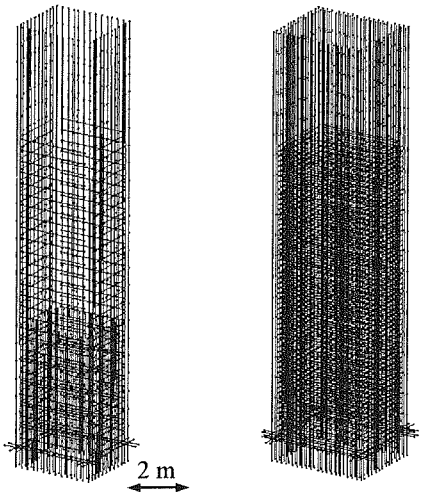

(a) S39 Pier (b) H8 Pier

Figure 12. Reinforcement detailing

Seismic performance evaluation with a dynamic analysis

Time-domain analysis results of piers S39 and H8 under the ground motion L2a and L2b are shown in Figure 15. The figure also shows the analytic result obtained from the equivalent single-degree-of-freedom analysis (SDOF). From the previous section analysis, pier S39 possesses a brittle shear failure. The yielding force in the equivalent SDOF model is set to be equal to the shear strength of the pier. The analytical result of pier S39 subjected to ground motion L2a from the proposed model shows that even shear crack starts to occur at the time 2s, the pier can still survive from the rest of input ground motion. However, some residual displacement was observed at the end of the analysis. L2b also causes the shear cracking in pier S39 at the time 2s but the pier collapse can be observed later due to a rebar cut-off as shown in Figure 16. By examining the result obtained from pier H8 subjected to L2a, only a little amount of residual displacement is observed from the proposed model when compared with the SDOF model. This implies that some longitudinal reinforcing bars are still in an elastic range and pull the pier back to its original position by their remaining restoring force. When L2b is applied to H8, the spalling of concrete and reinforcement buckling was observed. This causes the large amount of residual displacement in pier L2b. Although

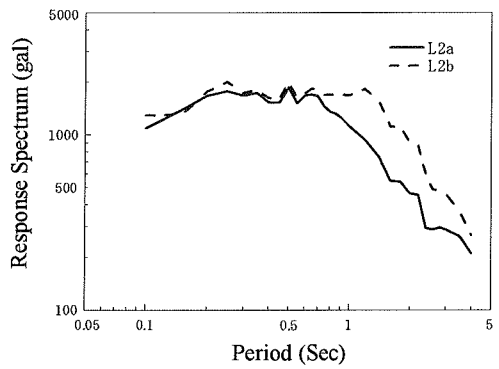

Figure 13. Acceleration spectra of earthquake ground motion L2a and L2b

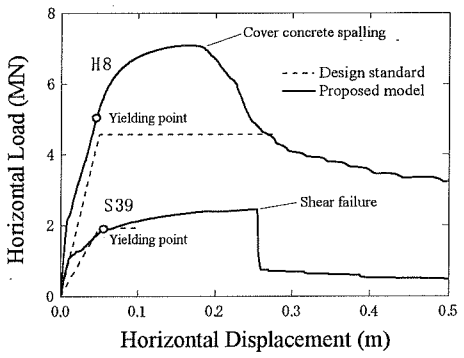

Figure 14. Static pushover analysis result of Pier S39 and H8

pier H8 did not collapse, the stability of the deck is questionable, especially when a simple span deck is used.

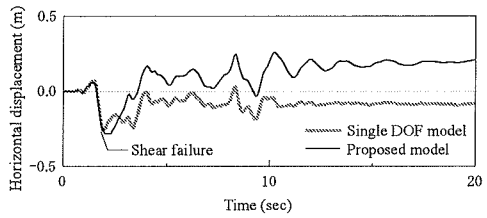

(a) Pier S39 subjected to L2a

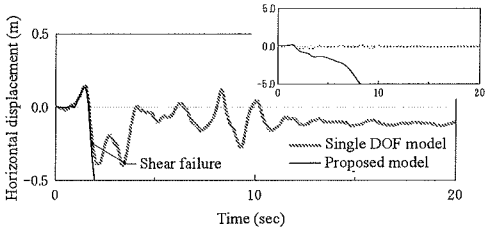

(a) Pier S39 subjected to L2b

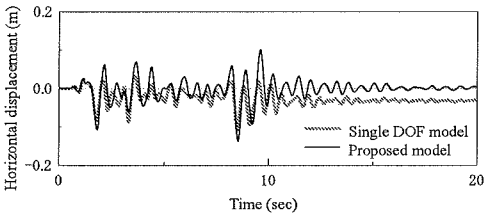

(c) Pier H8 subjected to L2a

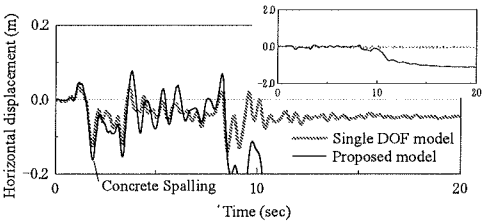

(c) Pier H8 subjected to L2b

Figure 15. Time-domain analysis response for displacement at the top of the pier

Seismic performance of the bridge with a simple span deck

The pier H8 was analyzed again here with the proposed model. Deck supports were considered as a roller on one side and a pin on the other. The input ground motion was applied in the direction of 45 degree relative to the deck. In case the pier subjected to L2a, although the reinforcement buckling occurred, L2a destructiveness is not high enough to cause a relative displacement that can make the bridge deck to fall down. On the other hand, a relatively high destructiveness of L2b results in reinforcement buckling and a large relative displacement at the roller support side. Regarding to this,

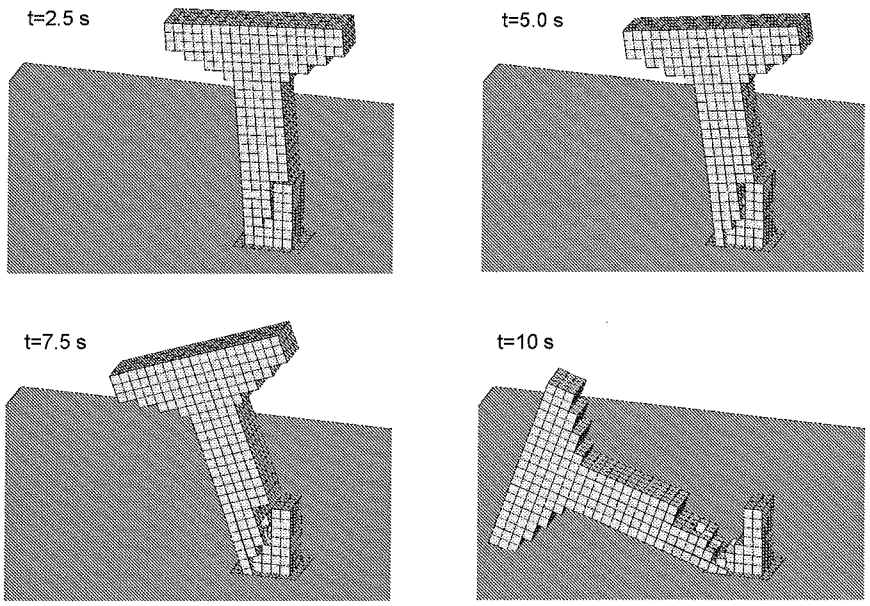

Figure 16. Collapse process of pier S39 subjected to ground motion L2b

the deck moved out of its support and fell down as shown in Figure 17.

CONCLUSION

An analytical model for collapse analysis takes into account the effect of post peak behavior due to reinforcement buckling and concrete spalling is developed. The analytical result was verified with the quasi-static static loading test result. The analysis of the pier designed with the 1964 Japan's seismic design code shows that brittle shear failure occurred even with the current design earthquake motion (the 1996 seismic design code). On the other hand, the pier designed by the current seismic code does not collapse although a ground motion exceeding the design standard was applied. In spite of this, the ground motion causes reinforcement buckling and the excessive residual displacement in the pier. By examining the bridge with a simple span deck, the relative displacement between the deck and the pier was found. If this displacement becomes large enough, the collapse of the deck can be observed.

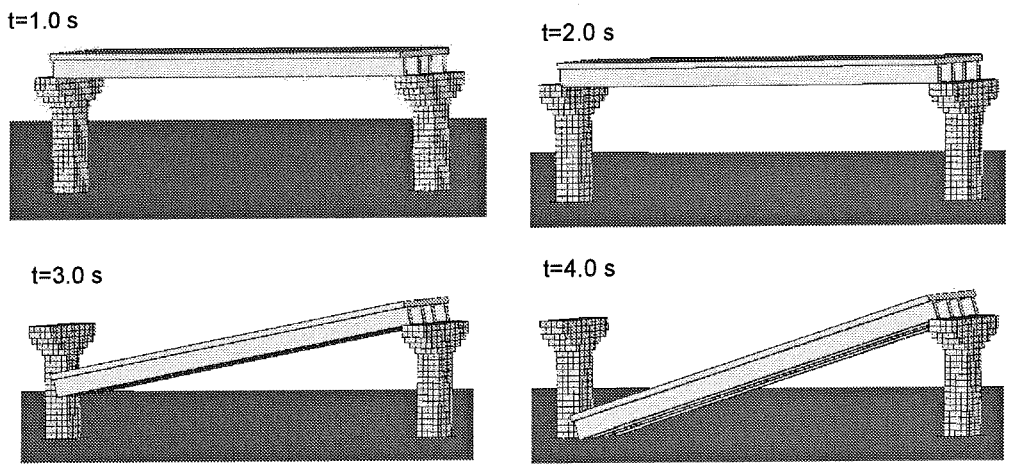

Figure 17. Collapse process of the bridge with a simple span deck

REFERENCES

Fukui J, Nakano M, Kimura Y, Ishida M, Okoshi M and Sakano A. (1998). "Loading tests about the ductility of pile foundations." *Technical Memorandum of PWRI.* Paper no. 3533.

Maekawa K, Pimanmas A and Okamura H. (2003). *Nonlinear mechanics of reinforced concrete*, Spon Press, London and New York.

Meguro K., and Hatem T. (2000). "Applied element method for structural analysis: theory and application for linear materials." *Journal of Structural Mechanics and Earthquake Engineering*, I-51, JSCE, 31-45.

Dhakal R. P and Maekawa K. (1999). "Post-peak cyclic behavior and ductility of reinforced concrete columns." Siminar *on Post-Peak Behavior of RC structures Subjected to Seismic Loads, Special Publication of JCI*, (JCI-C51E), 151-70.

Fukuura N, and Maekawa K. (1999). "Re-formulation of spatially averaged RC constitutive model with quasi-orthogonal bi-directional cracking." *Journal of Materials, Concrete Structures and Pavements*, 45(634), 157-76.

Kato B. (1979). "Mechanical properties of steel under load cycles idealizing seismic action." *CEB Bulletin D'Information,* 131, 7-27.

Suda K and Masukawa J. (1999). *Models for concrete cover spalling and reinforcement buckling of reinforced concrete, annual report*, Kajima Corporation, 47. (In Japanese)

Asatsu N, Unjoh S, Hoshikuma J and Kondoh M. (2001). "Plastic hinge length of reinforced concrete

columns based on the buckling characteristics of longitudinal reinforcement." *Journal of Structural Mechanics and Earthquake Engineering*, 682/I-56, JSCE, 177-194. (In Japanese)

Yoshikawa H. (2002). *Report of RC columns Tests*, Musashi Institute of Technology, 1997. (In Japanese)

JSCE. (2002). *Standard specifications for concrete structures-2002, seismic performance verification*, JSCE. (In Japanese)

Yoneda K, Kawashima K, Shogi G and Fujita Y. "Increase of seismic safety of an overcrossing associated with improvement of the seismic design codes." Journal of Structural Engineering 1993; 45A: 751-762. (In Japanese)